Superconducting nanowires: quantum confinement and spatially dependent Hartree–Fock potential

2009 J. Phys.: Condens. Matter 21 435701

(http://iopscience.iop.org/0953-8984/21/43/435701)

IOP Publishing Journal of Physics: Condensed Matter

J. Phys.: Condens. Matter **21** (2009) 435701 (7pp) doi:10.1088/0953-8984/21/43/435701

Superconducting nanowires: quantum confinement and spatially dependent Hartree–Fock potential

Yajiang Chen, M D Croitoru, A A Shanenko and F M Peeters

Departement Fysica, Universiteit Antwerpen, Groenenborgerlaan 171, B-2020 Antwerpen, Belgium

E-mail: arkady.shanenko@ua.ac.be

Received 7 August 2009
Published 8 October 2009
Online at stacks.iop.org/JPhysCM/21/435701

Abstract

It is well known that, in bulk, the solution of the Bogoliubov–de Gennes equations is the same whether or not the Hartree–Fock term is included. Here the Hartree–Fock potential is position independent and so gives the same contribution to both the single-electron energies and the Fermi level (the chemical potential). Thus, the single-electron energies measured from the Fermi level (they control the solution) stay the same. This is not the case for nanostructured superconductors, where quantum confinement breaks the translational symmetry and results in a position-dependent Hartree–Fock potential. In this case its contribution to the single-electron energies depends on the relevant quantum numbers. We numerically solved the Bogoliubov–de Gennes equations with the Hartree–Fock term for a clean superconducting nanocylinder and found a shift of the curve representing the thickness-dependent oscillations of the critical superconducting temperature to larger diameters.

(Some figures in this article are in colour only in the electronic version)

1. Introduction

Advances in nanofabrication technology resulted recently in high-quality metallic superconducting ultrathin nanofilms [1–4] and nanowires [5–8]. In most samples the electron mean free path was estimated to be about or larger than the nanofilm/nanowire thickness [2, 5, 8]. In this case the effects of the transverse quantization are not shadowed by impurity scattering and, hence, the conduction band splits up into a series of single-electron subbands resulting from the quantized transverse modes. This will have a pronounced effect on the superconducting properties (see, for instance [9, 10], and references therein). Notice that high-quality nanofilms do not exhibit significant indications of defect- or phase-driven suppression of superconductivity (see discussion in [2]). For high-quality nanowires the phase-fluctuation effects were shown to seriously influence the superconducting state only in narrowest aluminum specimens with width $\approx$ 5–8 nm [5, 8, 11]. Thus, the transverse quantum confinement is the major mechanism governing the superconducting properties in this case. Therefore, it is timely to study in a more detail clean nanosized superconductors in the presence of quantum confinement.

Quantum confinement breaks the translational symmetry and, so, the superconducting order parameter becomes position dependent. The well-known BCS ansatz for the ground state wavefunction is not applicable in this case, and the Bogoliubov–de Gennes (BdG) equations are a relevant tool to investigate equilibrium superconducting properties. Recent numerical studies of the BdG equations for nanofilms [9] and nanowires [10, 12, 13] show that the transverse quantum confinement has a substantial impact on the superconducting solution. However, the BdG equations investigated in [9, 10, 12, 13], were solved without the Hartree–Fock (HF) potential. The reason is that in bulk, the superconducting solution is not sensitive to the HF term in the BdG equations [14] and, so, the common expectation is that a similar conclusion holds for the broken translational symmetry. However, there is no detailed investigations on this subject and, so, such a study is needed.

In the bulk BdG equations, the HF potential is not spatially dependent and, so, it produces the same contribution to all

single-electron energies, with no dependence on the relevant quantum numbers. Hence, the Fermi level (the chemical potential) acquires the same contribution, as well, and the single-electron energies measured from the Fermi level are not changed. It is well known that the BdG equations are derived within the grand canonical formalism and, so, the electron energies appearing in the basic expressions absorb the chemical potential. As a result, the superconducting solution is insensitive to the HF potential. The situation is different in the presence of quantum confinement. The translational symmetry is now broken, the HF mean field is position dependent, and, so, its contribution to the single-electron energies depends on the relevant quantum numbers. Furthermore, the single-electron wavefunctions themselves are influenced by the presence of the HF field, i.e., an additional spatially dependent potential. Therefore, one can expect that the HF term in the BdG equations can change the superconducting solution in the presence of quantum confinement. It is of importance to clarify to what extent this will be through. In particular, this concerns the thickness-dependent oscillations (i.e., quantum-size oscillations) of the superconducting properties typical of high-quality nanofilms and nanowires [1, 2, 9, 10].

In the present work, by numerically solving the BdG equations for a superconducting clean nanocylinder, we investigate how the HF term influences the superconducting solution in the presence of quantum confinement.

The paper is organized as follows. In section 2 we outline the formalism of the BdG equations for a nanocylinder. In addition, Anderson's approximate semi-analytical solution to these equations is constructed here under the assumption that the single-electron wavefunctions do not change in the presence of the HF interaction. This makes it possible to check the effect of the HF field on the relevant wavefunctions. In section 3 we investigate and discuss numerical results of the BdG equations with and without the HF term and compare them with Anderson's approximation.

2. Bogoliubov–de Gennes equations and Anderson's recipe

We focus on the basic superconducting properties of a metallic clean cylindrical nanowire (with diameter $D = 2R$ and length L) in the quantum-size regime when the transverse quantization of the single-electron spectrum is of importance. In the presence of quantum confinement the translational invariance is broken, and the order parameter appears to be position dependent, i.e., $\Delta(\mathbf{r})$. It is well known that the BdG equations are a common and useful approach to investigate such a situation. Generally, these equations can be represented as follows:

$$E_\nu|u_\nu\rangle = \hat{H}_\mathrm{e}|u_\nu\rangle + \hat{\Delta}|v_\nu\rangle, \tag{1}$$

$$E_\nu|v_\nu\rangle = \hat{\Delta}^*|u_\nu\rangle - \hat{H}_\mathrm{e}^*|v_\nu\rangle, \tag{2}$$

where E_ν stands for the quasiparticle energy, $|u_\nu\rangle$ and $|v_\nu\rangle$ are the particle-like and hole-like ket vectors. In the clean limit the single-electron Hamiltonian in equations (1) and (2) is of the form (for zero magnetic field, $\mathbf{A} = 0$)

$$\hat{H}_\mathrm{e} = \hat{H}_\mathrm{e}^* = \frac{\hat{\mathbf{p}}^2}{2m_\mathrm{e}} + \Phi_\mathrm{HF}(\hat{\mathbf{r}}) + V_\mathrm{conf}(\hat{\mathbf{r}}) - E_\mathrm{F}, \tag{3}$$

with $\hat{\mathbf{r}}$ and $\hat{\mathbf{p}}$ the position and momentum operators, E_F the Fermi level, m_e the electron band mass (set to the free electron mass), $V_\mathrm{conf}(\mathbf{r})$ the confining interaction, and $\Phi_\mathrm{HF}(\mathbf{r})$ the HF potential. In bulk the confining interaction can be neglected and we arrive at the usual BCS picture based on plane waves. Below we adopt the simplest choice of the confining interaction potential: zero inside and infinite outside the wire. The gap-operator $\hat{\Delta}$ in equations (1) and (2) is related to the order parameter by $\hat{\Delta} = \Delta(\hat{\mathbf{r}})$.

As a mean-field theory, the BdG equations are solved in a self-consistent manner with the self-consistency relations given by

$$\Delta(\mathbf{r}) = g\sum_{\nu\in\mathcal{C}}\langle\mathbf{r}|u_\nu\rangle\langle v_\nu|\mathbf{r}\rangle[1-2f_\nu], \tag{4}$$

$$\Phi_\mathrm{HF}(\mathbf{r}) = -g\sum_{\nu}[|\langle\mathbf{r}|u_\nu\rangle|^2 f_\nu + |\langle\mathbf{r}|v_\nu\rangle|^2(1-f_\nu)], \tag{5}$$

where $g > 0$ is the coupling constant, $f_\nu = 1/(\mathrm{e}^{\beta E_\nu}+1)$ is the Fermi function ($\beta = 1/(k_\mathrm{B}T)$ with T the temperature and k_B the Boltzmann constant). In equation (4) $\mathcal{C}$ indicates the set of quantum numbers corresponding to the single-electron energy ξ_ν (measured from the Fermi level) located in the Debye window $\xi_{\nu\in\mathcal{C}} \in [-\hbar\omega_\mathrm{D}, \hbar\omega_\mathrm{D}]$ (ω_D is the Debye frequency), where ξ_ν absorbs the HF potential, i.e.,

$$\xi_\nu = \langle u_\nu|\hat{H}_\mathrm{e}|u_\nu\rangle + \langle v_\nu|\hat{H}_\mathrm{e}^*|v_\nu\rangle. \tag{6}$$

The cut-off in equation (4) is known [15] to be a payment for using a simplified delta-function approximation for the electron–electron interaction. Such a regularization is not needed in equation (5). For our confining interaction (i.e., zero inside and infinite outside) we have

$$\langle\mathbf{r}|u_\nu\rangle|_{\mathbf{r}\in S} = \langle\mathbf{r}|v_\nu\rangle|_{\mathbf{r}\in S} = 0 \tag{7}$$

at the sample surface, i.e., $\mathbf{r}\in S$. Periodic boundary conditions with unit cell L can be applied in the direction parallel to the nanowire.

The Fermi level (i.e., the chemical potential) is determined from

$$n_\mathrm{e} = \frac{2}{\pi R^2 L}\sum_{\nu}[\langle u_\nu|u_\nu\rangle f_\nu + \langle v_\nu|v_\nu\rangle(1-f_\nu)], \tag{8}$$

where n_e is the mean electron density. We use the BdG equations in the parabolic band approximation and, so, as discussed in [9], an effective Fermi level should be introduced, to recover the correct period of the quantum-size oscillations. For aluminum (the aluminum parameters are used below) $E_\mathrm{F} = 0.9$ eV for $D \approx 10$ nm (see [10]). For $D \sim 1$–2 nm, E_F shifts systematically from this value up, due to equation (8).

Due to the chosen confining geometry, it is convenient to use cylindrical coordinates ρ, φ and z. In this case the order parameter (the anomalous pairing potential) and HF mean field (the normal potential) depend only on the transverse coordinate, i.e., $\Delta(\rho)$ and $\Phi_\mathrm{HF}(\rho)$, and $\langle\mathbf{r}|u_\nu\rangle$ and $\langle\mathbf{r}|v_\nu\rangle$ are represented in the form ($\nu = \{j, m, k\}$)

$$\begin{pmatrix}\langle\mathbf{r}|u_{jmk}\rangle\\ \langle\mathbf{r}|v_{jmk}\rangle\end{pmatrix} = \frac{\mathrm{e}^{\mathrm{i}m\varphi}}{\sqrt{2\pi}}\frac{\mathrm{e}^{\mathrm{i}kz}}{\sqrt{L}}\begin{pmatrix}u_{jmk}(\rho)\\ v_{jmk}(\rho)\end{pmatrix}, \tag{9}$$

with j controlling the number of nodes in the transverse direction, m the azimuthal quantum number, and k the wavevector of the quasi-free electron motion along the nanocylinder. Inserting equation (9) into equations (1) and (2), we recast the BdG equations as

$$[E_{jmk} - \mathcal{L}_\rho - \Phi_{\rm HF}(\rho)]\, u_{jmk}(\rho) = \Delta(\rho) v_{jmk}(\rho), \tag{10}$$

$$[E_{jmk} + \mathcal{L}_\rho + \Phi_{\rm HF}(\rho)]\, v_{jmk}(\rho) = \Delta(\rho) u_{jmk}(\rho), \tag{11}$$

where $\Delta(\rho)$ is real, and

$$\mathcal{L}_\rho = -\frac{\hbar^2}{2m_{\rm e}}\left(\frac{\partial^2}{\partial\rho^2} + \frac{1}{\rho}\frac{\partial}{\partial\rho} - \frac{m^2}{\rho^2} - k^2\right) - E_{\rm F}. \tag{12}$$

The self-consistency relations can be rewritten as,

$$\Delta(\rho) = \frac{g}{2\pi L}\sum_{jmk\in C} u_{jmk}(\rho) v_{jmk}(\rho)[1 - 2f_{jmk}], \tag{13}$$

$$\Phi_{\rm HF}(\rho) = -\frac{g}{2\pi L}\sum_{jmk}[u^2_{jmk}(\rho) f_{jmk} + v^2_{jmk}(\rho)(1 - f_{jmk})], \tag{14}$$

with $u_{jmk}(\rho)$ and $v_{jmk}(\rho)$ real. To numerically solve equations (10) and (11), we expand the transverse particle-like and hole-like wavefunctions as

$$\begin{pmatrix} u_{jmk}(\rho) \\ v_{jmk}(\rho) \end{pmatrix} = \sum_J \begin{pmatrix} u_{jmk,J} \\ v_{jmk,J} \end{pmatrix} \vartheta_{Jm}(\rho), \tag{15}$$

with

$$\vartheta_{Jm}(\rho) = \frac{\sqrt{2}}{R\mathcal{J}_{m+1}(\alpha_{Jm})}\mathcal{J}_m\left(\alpha_{Jm}\frac{\rho}{R}\right), \tag{16}$$

where $\mathcal{J}_m(x)$ is the Bessel function of the first kind of the m-order, and α_{Jm} is the Jth zero of this function. This allows one to convert equations (10) and (11) into a matrix form. Then, a numerical solution can be obtained by diagonalizing the corresponding matrix, and self-consistency is reached by iterating equations (13) and (14). One should keep in mind that [15] $\langle u_\nu|u_\nu\rangle + \langle v_\nu|v_\nu\rangle = 1$ and, so,

$$\int_0^R {\rm d}\rho\, \rho[u^2_{jmk}(\rho) + v^2_{jmk}(\rho)] = 1. \tag{17}$$

As seen, the vector $(u_{jmk,J}; v_{jmk,J})^{\rm T}$ $(J = 0, 1, \ldots)$ is normalized.

In addition to the above procedure, below we use the Anderson approximate solution, as well [16]. Within this approximation, instead of the expansion given by equation (15), it is assumed that

$$u_{jmk}(\rho) = \mathcal{U}_{jmk}\,\vartheta_{jm}(\rho), \qquad v_{jmk}(\rho) = \mathcal{V}_{jmk}\,\vartheta_{jm}(\rho). \tag{18}$$

Equations (18) means that we seek a minimum of the BdG thermodynamic functional in the subspace of $u_{jmk}(\rho)$ and $v_{jmk}(\rho)$ proportional to the eigenfunctions of $\mathcal{L}_\rho$. Notice that it is possible to deal with Anderson's recipe, invoking the eigenfunctions of $\mathcal{L}_\rho + \Phi_{\rm HF}(\rho)$. However, below we are interested in equations (18) because it helps to clarify how a change in the single-electron wavefunctions due to the HF potential, can contribute to the problem of interest. To be accurate, the Anderson approximation should be based on the true single-electron wavefunctions. We recently found that in this case the error in Anderson's solution for $D \lesssim$ 2–3 nm is less than 1–2% [17]. Hence, comparing the results of numerically solving equations (10) and (11) with the data based on equations (18), we can reach unambiguous conclusions about the role of the changes in the single-electron wavefunctions due to the HF interaction. As follows from equations (18) (see, for instance, [17]), Anderson's approximation results in the BCS-like self-consistent equation

$$\Delta_{j'm'} = -\frac{1}{2}\sum_{jmk\in C}\frac{g_{j'm',jm}\Delta_{jm}}{\sqrt{\xi^2_{jmk} + \Delta^2_{jm}}}[1 - 2f_{jmk}], \tag{19}$$

with

$$\Delta_{jm} = \int_0^R {\rm d}\rho\, \rho\, \vartheta^2_{jm}(\rho)\Delta(\rho) \tag{20}$$

and the interaction-matrix element given by

$$g_{j'm',jm} = -\frac{g}{2\pi L}\int_0^R {\rm d}\rho\, \rho\vartheta^2_{j'm'}(\rho)\, \vartheta^2_{jm}(\rho). \tag{21}$$

For the single-electron energy appearing in equation (19) we have

$$\xi_{jmk} = \frac{\hbar^2}{2m_{\rm e}}\left[\frac{\alpha^2_{jm}}{R^2} + k^2\right] + \Phi_{jm} - E_{\rm F}, \tag{22}$$

where

$$\Phi_{jm} = \int_0^R {\rm d}\rho\, \rho\, \vartheta^2_{jm}(\rho)\Phi_{\rm HF}(\rho). \tag{23}$$

Inserting equation (5) into equation (23), one obtains

$$\Phi_{j'm'} = \frac{1}{2}\sum_{jmk} g_{j'm',jm}\left[1 - \frac{\xi_{jmk}(1 - 2f_{jmk})}{\sqrt{\xi^2_{jmk} + \Delta^2_{jm}}}\right]. \tag{24}$$

We should not forget about $E_{\rm F}$ appearing in the single-electron energy given by equation (22). It is fixed through equation (8) that is now of the form

$$n_{\rm e} = \frac{1}{\pi R^2 L}\sum_{jmk}\left[1 - \frac{\xi_{jmk}(1 - 2f_{jmk})}{\sqrt{\xi^2_{jmk} + \Delta^2_{jm}}}\right]. \tag{25}$$

Thus, in the Anderson approximation introduced by equations (18), one needs to solve equations (19) and (24), keeping equation (25). As already mentioned above, comparing a numerical solution of equations (10) and (11) with the solution based on Anderson's recipe, we can check the effect of the HF interaction on the single-electron wavefunctions.

3. Numerical results

In this section we investigate and discuss numerical self-consistent solutions of equations (10) and (11) with the HF potential (the full version) and without it (the truncated version, by setting $\Phi_{\rm HF}(\rho) = 0$ in the relevant expressions). Results are also compared with a solution of equations (19) and (24). All the calculations are performed with the parameters typical

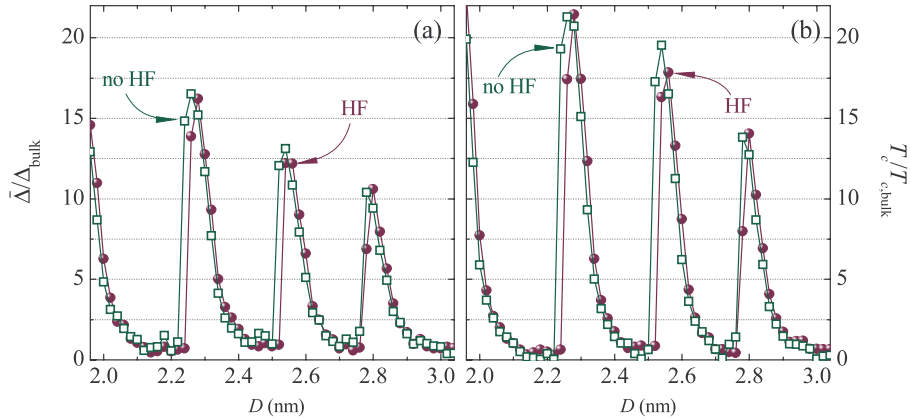

Figure 1. (a) The spatially averaged superconducting order parameter $\bar{\Delta}/\Delta_{\rm bulk}$ and (b) critical temperature $T_{\rm c}/T_{\rm c,bulk}$ versus the nanowires diameter D as calculated from the BdG equations (10) and (11) at zero temperature.

for aluminum [15, 14]: $\hbar\omega_{\rm D} = 32.31$ meV; $gN(0) = 0.18$, with $N(0) = m_{\rm e}k_{\rm F}/(2\pi^2\hbar^2)$ the bulk density of single-electron states at the Fermi level (for $E_{\rm F}$ see discussion after equation (8)) and $k_{\rm F}$ the bulk Fermi wavevector. For these parameters the bulk BCS coherence length $\xi_0 = 1.6\ \mu$m is significantly larger than the nanocylinder diameter. However, contrary to the ordinary Ginzburg–Landau picture, the superconducting order parameter now exhibits significant spatial variations in the transverse direction due to the broken translational symmetry. The length of the nanocylinder is taken as $L = 1\ \mu{\rm m} \gg \lambda_{\rm F} = 2\pi/k_{\rm F}$. This is an optimal choice, upholding, on one side, the use of periodic boundary conditions in the z direction and, on the other side, it results in a reasonable calculational time. As opposed to the truncated BdG equations, their full version requires much more time for convergence of the numerical procedure, and this time increases proportionally with L^2. Numerically solving the Anderson equations (19) and (24) is less time-consuming and, so, we take $L = 5\ \mu$m in this case.

In figure 1(a) the spatially averaged order parameter

$$\bar{\Delta} = \frac{2}{R^2}\int_0^R {\rm d}\rho\,\rho\Delta(\rho),$$

calculated from equations (10) and (11), is plotted in units of the bulk order parameter ($\Delta_{\rm bulk} = 0.25$ meV) versus the nanocylinder diameter with and without the HF mean field. In figure 1(b) the corresponding critical temperature $T_{\rm c}$ (in units of the bulk one) is given. As seen, both data-sets exhibit pronounced size-dependent oscillations, typical of high-quality superconducting nanofilms and nanowires with uniform thickness [1, 2, 9, 10]. Such oscillations result from single-electron subbands forming due to the transverse quantization of the electron motion. With an increase in the nanowire diameter, the subbands shift down in energy. Each time when a new subband comes into the Debye window around the Fermi level, the number of single-electron states contributing to the superconducting order parameter increases, and a size-dependent superconducting resonance develops. As follows from figure 1, the quantum-size oscillations corresponding to the full version of the BdG equations are somewhat shifted up. The mean distance between neighboring superconducting resonances is controlled by the bulk Fermi wavelength $\lambda_{\rm F}$ and, so, the shift magnitude is roughly proportional to $\lambda_{\rm F}$. For typical metallic parameters this magnitude is about the unit-cell dimensions. However, for low-carrier-density materials, e.g., superconducting semiconductors (see, for instance [18–21], and recent papers on boron-doped diamond [22, 23] and boron-doped silicon [24]), such a shift can approach the scale of few nanometers. The difference between the two sets of data in figure 1 is most significant for those diameters, where a size-dependent superconducting resonance in the case without the HF interaction is already present while in the full version such a resonance only starts to develop. The difference is not so significant but still survive when the resonance comes into its decay stage. When the resonance is fully decayed (the off-resonant regime), the HF corrections are practically negligible, and we arrive at the situation similar to bulk. Notice that small differences between the numerical results of the full and truncated BdG equations in the off-resonant regime (due to beating patterns of the corresponding curves), are because of the chosen nanowire length. Indeed, as follows from calculations for several selected off-resonant diameters, such beating patterns disappear when L increases up to 20–30 μm, and the results with and without the HF interaction approach each other.

Notice that maxima of $T_{\rm c}/T_{\rm c,bulk}$ in figure 1(b) are generally higher than those of $\bar{\Delta}/\bar{\Delta}_{\rm bulk}$ in figure 1(a). This is due to formation of new Andreev-type states induced by the transverse quantum confinement (see details in [25]), which results in a decrease of $\bar{\Delta}/(k_{\rm B}T_{\rm c})$ below the bulk value 1.763 at the resonant points. As seen from figure 1, inclusion of the HF interaction can slightly reduce the resonant enhancements, with practically no effect on the ratio $\bar{\Delta}/(k_{\rm B}T_{\rm c})$.

In figure 2 we present different quantities calculated with the full and truncated versions of equations (10) and (11) for two diameters: the upper panel, for $D = 2.24$ nm; and the lower panel, for $D = 2.6$ nm. The upper panel represents the situation when a superconducting resonance is developed for the truncated version but is not yet present for the full version of the BdG equations. In figure 2(a) the superconducting order parameter $\Delta(\rho)$ calculated with (HF) and without the HF

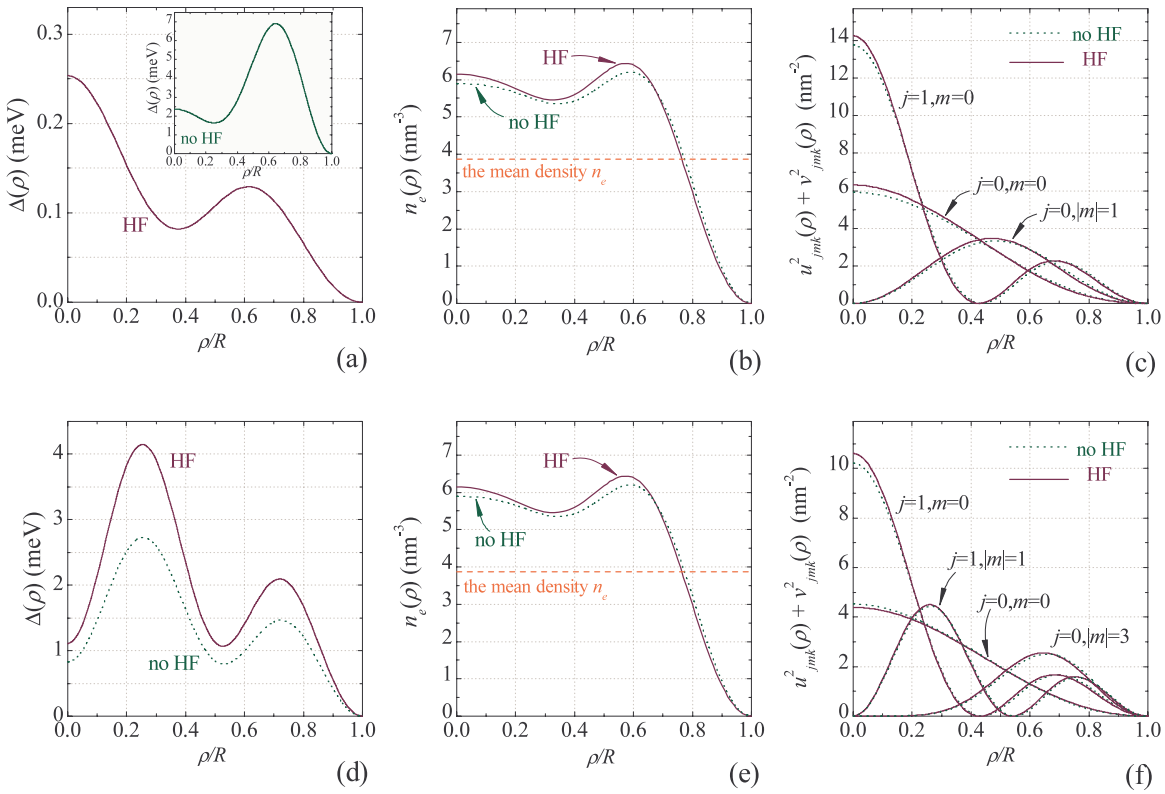

Figure 2. Upper panel: (a) the superconducting order parameter $\Delta(\rho)$, (b) the local density $n_e(\rho)$ and (c) the distribution $u^2_{jmk}(\rho)+v^2_{jmk}(\rho)$ versus ρ/R for $D = 2.24$ nm. The lower panel: the same but for $D = 2.6$ nm. The results for the truncated (no HF) and full (HF) BdG equations are plotted.

interaction (no HF, the inset), is plotted versus the transverse coordinate ρ/R for $T = 0$. The spatial distribution of the pair condensate is very different for these two cases: the data without the HF interaction are larger by an order of magnitude, and even the profile of $\Delta(\rho)$ is different. In figure 2(b) the local electron density, i.e.,

$$n_e(\rho) = \frac{1}{\pi L}\sum_{jmk}[u^2_{jmk}(\rho)f_{jmk} + v^2_{jmk}(\rho)(1-f_{jmk})], \quad (26)$$

is shown for the same diameter. As can be expected, now the difference between the two data-sets is not so significant (we keep to the same value of the mean electron density n_e). Due to the attractive character of the effective electron–electron interaction, the HF potential forces electrons to go closer to the nanocylinder center. However, the confining interaction has the major effect on $n_e(\rho)$ as compared to the HF potential producing only some small corrections. From the results for the local electron density, it is possible to expect that the single-electron wavefunctions are also not very sensitive to the HF interaction. For nanowires, $|u_\nu(\mathbf{r})|$ and $|v_\nu(\mathbf{r})|$ is nearly proportional to the corresponding single-electron wavefunction (see discussion above, after equations (18)). Hence, due to equation (17), the quantity $u^2_{jmk}(\rho)+v^2_{jmk}(\rho)$ can provide us with the information about the single-electron distribution. In figure 2(c) $u^2_{jmk}(\rho)+v^2_{jmk}(\rho)$ is plotted versus ρ/R for the quantum numbers most sensitive to including the HF interaction. We can indeed see that the effect of the HF potential on the wavefunctions is minor. Similar conclusions can be obtained from the lower panel of figure 2. The only exception is that the superconducting order parameter in figure 2(d) ($D = 2.6$ nm) does not change so much when including the HF potential. Notice that $n_e(\rho)$ given in figure 2(e) is practically the same as in figure 2(b). However, this is not true for $u^2_{jmk}(\rho)+v^2_{jmk}(\rho)$ (compare panel (c) with panel (f)). The point is that the integral $\int_0^R \mathrm{d}\rho\,\rho\,n_e(\rho) = n_e R^2/2$ changes with the radius but for the single-electron distribution $u^2_{jmk}(\rho)+v^2_{jmk}(\rho)$ we have equation (17).

From the results presented in figure 2, one expects minor effects on the single-electron wavefunctions due to the incorporation of the HF interaction. This expectation can be put on a more solid ground by using the Anderson approximation based on equations (19) and (23). We remind that the Anderson approximation is quite good for superconducting nanowires provided that it involves the true single-electron wavefunctions. Equations (19) and (23) follow from equations (18) and, hence, as assumed, the single-electron wavefunctions are not altered by our position-dependent HF interaction. If this is a reasonable assumption, results of the Anderson approximation constructed in this way, should be close to the results of the full BdG equations. As seen from figure 3, this is indeed the case. We can conclude that the thickness-dependent shift of the superconducting resonances in the presence of the HF interaction has nothing to do with the single-electron wavefunctions. Its mechanism is due to the fact

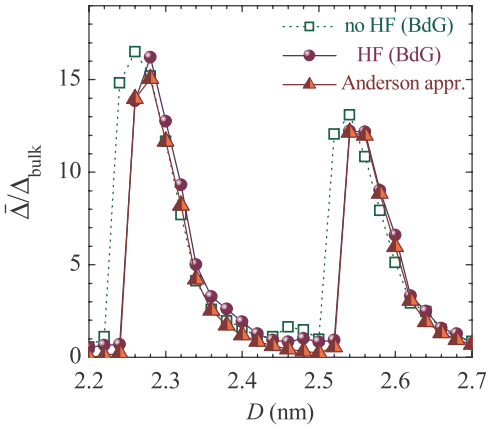

Figure 3. $\bar{\Delta}/\Delta_{\rm bulk}$ versus the nanowire diameter ($T = 0$): triangles correspond to the Anderson approximation (the HF field is included); circles and squares are the numerical results of the full and truncated BdG equations, respectively.

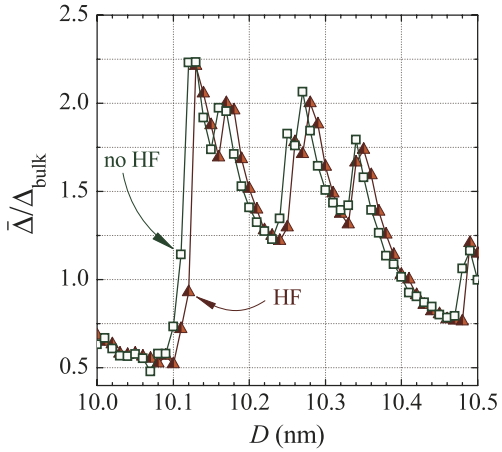

Figure 4. HF versus no HF: $\bar{\Delta}/\Delta_{\rm bulk}$ as a function of the nanowire diameter D at zero temperature (squares are the results of the truncated BdG equations (no HF interaction); triangles are the results of the Anderson approximation, see equations (19) and (23)).

that the position-dependent HF potential results in a change of the single-electron energies measured from the Fermi level.

So far we considered extremely narrow nanowires, for the sake of simplicity. However, a similar shift (≈0.01–0.02 nm) of the quantum-size oscillations due to the HF term survives until the total decay of the quantum-size oscillations (up to diameters of about 50–70 nm). In particular, such a shift is clearly seen in figure 4, where numerical results of the truncated BdG equations for $D = 10$–10.5 nm are compared with a solution of equations (19) and (23) including the HF potential. Thus, we arrive at the following picture. In the vicinity of a superconducting resonance, the bottom of some single-electron subband is situated close to the Fermi level. Therefore, a repositioning of this subband with respect to the Fermi level can result in a significant change of the number of single-electron states in the Debye window and, so, in a remarkable increase/decrease of superconducting characteristics. However, when bottoms of all single-electron subbands are quite apart from the Fermi level, i.e., in the off-resonant regime, a move of these subbands in energy produces much less important effect on the number of single-electron states located in the Debye window. This is why the decay of a superconducting resonance is accompanied by a depletion of the influence of the HF potential.

4. Conclusions

Quantum confinement breaks the translational symmetry in nanostructured superconductors. In this case, despite the delta-function approximation for the electron–electron interaction, the HF potential becomes position dependent, and its contribution to the single-electron energy (measured from the Fermi level) is a function of the relevant quantum numbers (contrary to bulk!). By numerically solving the Bogoliubov–de Gennes equations for a clean metallic nanocylinder, we have shown that such a feature results in a shift of the curve representing the thickness-dependent oscillations of the critical temperature (the energy gap, the order parameter etc) to larger diameters. For metallic parameters it is of about the typical unit-cell dimensions. Notice that this is quite enough to completely change the pattern of thickness-dependent oscillations of T_c between the Pb nanofilms with even and odd numbers of monolayers (see [1, 3, 4]). For low-carrier-density materials, e.g., superconducting semiconductors, such a shift increases significantly (proportionally to the relevant Fermi wavelength) and can reach the scale of few nanometers or even larger.

Acknowledgments

Yajiang Chen thanks B Xu and R Geurt for helpful discussions. This work was supported by the Flemish Science Foundation (FWO-Vl), the Belgian Science Policy (IAP) and ESF-AQDJJ network.

References

[1] Guo Y, Zhang Y-F, Bao X-Y, Han T-Z, Tang Z, Zhang L-X, Zhu W-G, Wang E G, Niu Q, Qiu Z Q, Jia J-F, Zhao Z-X and Xue Q K 2004 *Science* **306** 1915

[2] Özer M M, Thompson J R and Weitering H H 2006 *Nat. Phys.* **2** 173
Özer M M, Thompson J R and Weitering H H 2006 *Phys. Rev.* B **74** 235427
Özer M M, Jia Y, Zhang Z, Thompson J R and Weitering H H 2007 *Science* **316** 1594

[3] Eom D, Qin S, Chou M-Y and Shih C K 2006 *Phys. Rev. Lett.* **96** 027005

[4] Qin S, Kim J, Niu Q and Shih C-K 2009 *Science* **324** 1314

[5] Savolainen M, Touboltsev V, Koppinen P, Riikonen K-P and Arutyunov K 2004 *Appl. Phys.* A **79** 1769
Zgirski M, Riikonen K-P, Touboltsev V and Arutyunov K 2005 *Nano Lett.* **5** 1029
Zgirski M, Riikonen K-P, Tuboltsev V, Jalkanen P P, Hongisto T T and Arutyunov K Y 2008 *Nanotechnology* **19** 055301

[6] Tian M L, Wang J G, Kurtz J S, Liu Y, Chan M H W, Mayer T S and Mallouk T E 2005 *Phys. Rev.* B **71** 104521

[7] Jankovič L, Gournis D, Trikalitis P N, Arfaoui I, Cren T, Rudolf P, Sage M-H, Palstra T T M, Kooi B, De Hosson J, Karakassides M A, Dimos K, Moukarika A and Bakas T 2006 *Nano Lett.* **6** 1131
Tombros N, Buit L, Arfaoui I, Tsoufis T, Gournis D, Trikalitis P N, van der Molen S J, Rudolf P and van Wees B J 2008 *Nano Lett.* **8** 3060
[8] Altomare F, Chang A M, Melloch M R, Hong Y and Tu C W 2006 *Phys. Rev. Lett.* **97** 017001
[9] Shanenko A A, Croitoru M D and Peeters F M 2006 *Europhys. Lett.* **76** 498
Shanenko A A, Croitoru M D and Peeters F M 2007 *Phys. Rev.* B **75** 014519
[10] Shanenko A A and Croitoru M D 2006 *Phys. Rev.* B **73** 012510
Shanenko A A, Croitoru M D, Zgirski M, Peeters F M and Arutyunov K 2006 *Phys. Rev.* B **74** 052502
[11] Arutyunov K Yu, Golubev D S and Zaikin A D 2008 *Phys. Rep.* **464** 1
[12] Han J E and Crespi V H 2004 *Phys. Rev.* B **69** 214526
[13] Grigorenko I, Zhu J-X and Balatsky A 2008 *J. Phys.: Condens. Matter* **20** 195204
[14] Fetter A L and Walecka J D 2003 *Quantum Theory of Many-Particle Systems* (New York: Dover)
[15] de Gennes P G 1966 *Superconductivity of Metals and Alloys* (New York: Benjamin)
[16] Anderson P W 1959 *J. Phys. Chem. Solids* **11** 26
[17] Shanenko A A, Croitoru M D and Peeters F M 2008 *Phys. Rev.* B **78** 024505
Shanenko A A, Croitoru M D and Peeters F M 2008 *Phys. Rev.* B **78** 054505
[18] Hein R A, Gibson J W, Mazelsky R, Miller R C and Hulm J K 1964 *Phys. Rev. Lett.* **12** 320
[19] Schooley J F, Hosler W R and Cohen M L 1964 *Phys. Rev. Lett.* **12** 474
Schooley J F, Hosler W R, Ambler E, Becker J H, Cohen M L and Koonce C S 1965 *Phys. Rev. Lett.* **14** 305
[20] Tavger B A and Demihovskii V Yu 1965 *Sov. Phys.—JETP* **21** 494
[21] Eagles D M 1967 *Phys. Rev.* **164** 489
[22] Ekimov E A, Sidorov V A, Bauer E D, Mel'nik N N, Curro N J, Thompson J D and Stishov S M 2004 *Nature* **428** 542
[23] Takano Y, Nagao M, Sakaguchi I, Tachiki M, Hatano T, Kobayashi K, Umezawa H and Kawarada H 2004 *Appl. Phys. Lett.* **85** 2851
[24] Bustarret E, Marcenat C, Achatz P, Kačmarčik J, Levy F, Huxley A, Ortega L, Bourgeois E, Blase X, Debarre D and Boulmer J 2006 *Nature* **444** 427
[25] Shanenko A A, Croitoru M D, Mints R G and Peeters F M 2007 *Phys. Rev. Lett.* **99** 067007